



**HAL**  
open science

# Effect of the injection of water-containing diluents on band broadening in analytical supercritical fluid chromatography

Magali Batteau, Karine Faure

► **To cite this version:**

Magali Batteau, Karine Faure. Effect of the injection of water-containing diluents on band broadening in analytical supercritical fluid chromatography. *Journal of Chromatography A*, 2022, 1673, pp.463056. 10.1016/j.chroma.2022.463056 . hal-03711565

**HAL Id: hal-03711565**

**<https://hal.science/hal-03711565v1>**

Submitted on 20 Oct 2022

**HAL** is a multi-disciplinary open access archive for the deposit and dissemination of scientific research documents, whether they are published or not. The documents may come from teaching and research institutions in France or abroad, or from public or private research centers.

L'archive ouverte pluridisciplinaire **HAL**, est destinée au dépôt et à la diffusion de documents scientifiques de niveau recherche, publiés ou non, émanant des établissements d'enseignement et de recherche français ou étrangers, des laboratoires publics ou privés.

# 1 Effect of the injection of water-containing diluents on band broadening in analytical 2 supercritical fluid chromatography

3  
4 Magali Batteau<sup>1</sup>, Karine Faure<sup>1</sup>

5 <sup>1</sup>Université de Lyon, CNRS, Université Claude Bernard Lyon 1, Institut des Sciences Analytiques,  
6 UMR 5280, 5 rue de la Doua, F-69100 VILLEURBANNE, France

7 \*Corresponding author: [karine.faure@isa-lyon.fr](mailto:karine.faure@isa-lyon.fr)  
8  
9

## 10 Abstract

11 In this study, the impact of introducing water in the sample solvent upon the injection in SFC is  
12 investigated. Adsorption of water on the stationary phase was indicated. Using a set of ten neutral test  
13 compounds and four ionizable test compounds, spread all along the co-solvent gradient, several  
14 parameters were scrutinized (i.e. water content in the sample diluent, nature of the sample diluent,  
15 nature of the co-solvent) in regards to peak broadening. From this systematic investigation, the  
16 competition for adsorption on the stationary phase between the analytes and the water molecules  
17 contained in the diluent was highlighted. The chromatographic peaks of neutral molecules eluting  
18 before water molecules were compressed and the ones eluting after were broadened. While the extent  
19 of this phenomenon was related to the peak position for neutral molecules, it was not observed on  
20 acidic molecules.

## 21 Keywords

22 Supercritical fluid chromatography; sample diluent; injection; peak broadening  
23  
24

## 25 1. Introduction

26 In analytical SFC, the injection is performed after the co-solvent and the CO<sub>2</sub> are mixed at initial  
27 proportions. Hence the injection plug is located in a zone usually rich in CO<sub>2</sub> and a viscosity mismatch  
28 is frequent. Moreover, the nature of the sample diluent is of major importance on the peak shape. The  
29 selection of the sample diluent is hence of great concern. For polar SFC stationary phases, aprotic  
30 and low viscosity solvents, such as MtBE, are recommended to avoid the formation of viscous  
31 fingering as well as any strong solvent effects [1].

32 However, for the past few years, the application area of SFC is growing interest towards more polar  
33 solutes which may experience solubility issues in aprotic solvents. The use of polar co-solvents in SFC  
34 eases the analysis of polar metabolites, sugars or peptides [2], for which water is usually the best  
35 solubilizing diluent. Another interesting development for SFC is its implementation as a second  
36 dimension in a two-dimensional chromatographic separation. This combination opens new  
37 opportunities, thanks to the large orthogonality it provides [3, 4], while it may impose the transfer of  
38 hydro-organic fractions into the SFC dimension.

39 The presence of water and eventually MeOH is known to be highly detrimental to SFC peak shapes,  
40 as these solvents both present elevated viscosity and polarity, contrasting with the initial CO<sub>2</sub>-rich  
41 mobile phase. So far, solutions consisted in injecting very low sample volumes. But Enmark et al.

42 highlighted that deformations can even happen at very low injection volume, starting at 0.3 % column  
43 volume [5]. Using specific flow-through needle injectors that increment the sample plug with a feed  
44 solvent has shown recently to be able to reduce the impact of MeOH diluent on the separation [6], but  
45 water as a diluent was not investigated. On the other hand, the situation where SFC is online with an  
46 LC instrument is even more demanding. In an online LC x SFC configuration, loops of large volume  
47 need to be used to allow sufficient time for the <sup>2</sup>D separation to be conducted. Moreover, the loops  
48 need to be fully filled to avoid residual air gaps, that may result from the decompression of the <sup>2</sup>D  
49 mobile phase in the loop, to be injected [7]. This leads to the injection of a large amount of <sup>1</sup>D mobile  
50 phase into the <sup>2</sup>D SFC dimension. Previous online hyphenation of LC with SFC avoided the water  
51 injection issue by removing the LC eluent through packed loop interfaces [8-10], or by injecting very  
52 low volumes into the SFC column [7]. While the first solution is highly effective, the risk of carry-over  
53 exists. On the other hand, the transfer of low volume is quite demanding in online two-dimensional  
54 separations, imposing a drastic reduction of the <sup>1</sup>D flow-rate. A better understanding of water impact  
55 upon injection in SFC is hence required.

56 Lastly, one can notice that studies focusing on injection effects of water-containing diluents in SFC  
57 have been performed under isocratic mode so far [5, 7, 11]. However, gradient elution is known to  
58 favor robustness in SFC [12] and is increasingly applied to separate analytes covering a wider range  
59 of polarity [13].

60 The goal of this experimental study was to conduct a systematic investigation of the influence of  
61 several parameters on band broadening when injecting samples dissolved in a water-containing  
62 diluent. These parameters included the position of the analyte peak, the water content in the injection  
63 solvent as well as the nature of the organic solvent injected along. The nature of the co-solvent and  
64 the presence of additives in this co-solvent were also investigated.

65

## 66 **2. Materials and methods**

### 67 **2.1 Chemicals, reagents and columns**

68 All standards had a purity exceeding 95%. The following standards were obtained from Sigma Aldrich  
69 (Germany): eugenol, 2,4,6-trimethylphenol, 1-indanol, apocynin, o-cresol, m-cresol, phenol, 4-  
70 hydroxybenzyl alcohol, naringenin, acrylic acid, imipramine hydrochloride and propranolol  
71 hydrochloride. Arbutin, trans-cinnamic acid and ferulic acid were obtained from Fluka (UK), Sigma  
72 Acros Organic (USA) and Sarsyntex (France), respectively.

73 Methanol (MeOH) ( $\geq 99.8\%$ ), ethanol ( $> 98\%$ ) and formic acid ( $> 98\%$ ) were purchased from Fisher  
74 Scientific (UK), acetonitrile (ACN) ( $\geq 99.9\%$ ) was purchased from Honeywell (Germany), methyl tert-  
75 butyl ether (MtBE) ( $\geq 99.9\%$ ) was purchased from Acros Organics (USA).

76 Ultrapure water was delivered by PURELAB Classic system from Elga (UK) (18.2 M $\Omega$ -cm).  
77 Ammonium hydroxide solution was ACS reagent (28.0-30.0 % NH<sub>3</sub> basis) purchased from Sigma-  
78 Aldrich (Germany). Pressurized carbon dioxide (CO<sub>2</sub>) (N45,  $\geq 99,995\%$ ) was purchased from Air  
79 Liquide (France).

80 Three columns were assessed, Torus DEA and Torus Diol with dimensions 100 x 3.0 mm, 1.7  $\mu$ m and  
81 BEH HILIC with dimensions 100 x 2.1 mm; 1.7  $\mu$ m, all from Waters (Milford, USA).

## 82 **2.2 SFC instrument**

83 All experiments were performed on an Agilent 1260 Infinity II SFC (Agilent, USA) equipped with a  
84 SFC-binary pump (G4782A), an oven column 1260 MCT (G7116A), a detector 1260 DAD WR  
85 (G7115A) equipped with a SFC flow cell (400 bars, 2  $\mu\text{L}$ , 3 mm path length) and a 1260 SFC control  
86 module (G4301A). To mimic the full loop injection that may occur during online LC x SFC, the  
87 commercial flow-through needle (FTN) injector was reverted to a fixed-loop model. The instrument  
88 was modified to accommodate a SFC-Autosampler (G4303A) with a fixed injection loop of either 5  $\mu\text{L}$ ,  
89 10  $\mu\text{L}$  or 20  $\mu\text{L}$  volume. The instrumental variance due to extra column was estimated at 37  $\mu\text{L}^2$  (liquid  
90 conditions) and at 12  $\mu\text{L}^2$  (for 5 % co-solvent). The dwell volume, excluding loop volume, was 780  $\mu\text{L}$ .

## 91 **2.3 Sample preparation**

92 A stock solution of each standard was prepared at 20 mg/mL or 20  $\mu\text{L}/\text{mL}$  in MeOH. Using the stock  
93 solutions, a mixture containing several compounds at a final concentration between 0.05 to 0.2 mg/mL  
94 (according to their UV response) in either MtBE, or ACN/water with various ratio, or MeOH /water with  
95 various ratio, except for imipramine prepared at 1 mg/mL.

## 96 **2.4 Chromatographic conditions**

97 Samples were injected with an injection volume of 5  $\mu\text{L}$ , 10  $\mu\text{L}$  or 20  $\mu\text{L}$  (full loop with overfill factor  
98 x2). The flow rate was 1.4 mL/min, so that the instrumental pressure remains below 400 bars during  
99 gradient. The initial composition of the mobile phase was 95 %  $\text{CO}_2$  / 5 % organic co-solvent (v/v), with  
100 a linear gradient up to a final composition of 50 % co-solvent, with a gradient time of 5.3 min  
101 (normalized gradient slope of 2 %). Then the column returned to the initial composition in 0.3 min  
102 (corresponding to one void volume) and was reconditioned with initial conditions for 2 min. Back-  
103 pressure was maintained constant at 140 bar. The column oven temperature was set at 40  $^{\circ}\text{C} \pm 0.8$   
104  $^{\circ}\text{C}$ . UV detection was set at 220 nm (bandwidth 4 nm, frequency 40 Hz) unless stated otherwise. The  
105 instrument was controlled by OpenLab CDS ChemStation C01.08 (Agilent). Ammonium hydroxide (20  
106 mM) was added to the co-solvent to avoid peak tailing when analysing basic compounds [14].  
107

## 108 **2.5 Selection of test compounds and column.**

109 While most studies on injection effect focus on poorly retained analytes, it seemed important to select  
110 compounds across the whole elution range while limiting the number of variables. A set of 10 neutral  
111 test compounds, with log P ranging from -0.6 to 2.2 was investigated, selected among lignin-derived  
112 compounds. Two smaller sets containing three acidic compounds and two basic compounds  
113 completed the study (Table 1).

114  
115 Diethylamine column (DEA) was selected as providing the largest elution range and resolution for the  
116 selected test compounds. Conditions of pressure and temperature in gradient SFC have been  
117 selected to be representative of the conditions the most used in literature, while offering the largest  
118 retention range [15, 16].

119 A non-linear density increase and a pressure gradient along the run at fixed BPR pressure (here 140  
120 bars) results in a dependency of retention behavior not only to gradient conditions (initial composition,

121 slope) but also to the operating conditions [17, 18]. For any rigorous method transfer of a linear  
122 gradient, solute retention should be reported via composition at elution expressed as co-solvent  
123 molarity [19, 20]. Nonetheless, for easiness of instrumental setup, the apparent composition at elution  
124 (Eq. 1), expressed in volumetric fraction of co-solvent was used throughout this study. This  
125 straightforward comparison of elution of analytes is possible, as all experiments were performed on a  
126 single instrumentation with highly repeatable pressure profile throughout the runs.

127

128 The composition at elution,  $C_e$ , was given by:

$$129 \quad C_e = C_i + \frac{C_f - C_i}{t_g} \times (t_R - t_0 - t_D) \quad (1)$$

130 with  $t_R$  the compound retention time and  $t_D$  the instrument dwell time.

131  $C_i$  and  $C_f$  are the initial and final eluent compositions expressed as volumetric fractions,  $t_g$  the gradient  
132 time and  $t_0$  the column dead time. The dwell time was determined by performing a triplicate set of  
133 gradient profiles without column, with a gradient composition ranging from 60% to 85 % co-solvent. A  
134 larger compositional range led to non-linear absorbance profile.

135

### 136 **3. Results and discussion**

137 This study has been carried out using generic SFC conditions with a gradient elution from 5 % to 50 %  
138 co-solvent and a set of neutral, acidic and basic test compounds.

139 Methyl tert-butyl ether (MtBE) is considered as a very weak solvent and the variance generated by the  
140 injection in this solvent is considered close to the one generated by heptane, while allowing  
141 compounds of a wide range of polarity to be soluble [1]. Hence it was considered through this study as  
142 the reference injection solvent. Figure 1 shows the reference chromatogram, with MeOH as co-  
143 solvent, when injecting the test compounds diluted in 5  $\mu$ L MtBE. The retention times and hence the  
144 apparent composition at elution of the test compounds are reported in Table 1. Because of the large  
145 dwell volume (1.8 times the column volume), three compounds eluted on the resulting isocratic step, at  
146 the initial composition of 5 % MeOH, with retention factor ranging from 0.8 to 1.3. These compounds  
147 had a smaller column dispersion contribution and hence were expected to be highly influenced by  
148 injection effects, besides instrumental variance. Then the next seven neutral test compounds eluted in  
149 the range of 6 % to 35 % MeOH. Retention times were repeatable with intermediate precision (5 days)  
150 reaching 2.0 % RSD for the low retained test compounds and 1.3 % RSD for the test compounds  
151 eluting during the gradient.

152 Because the viscosity and pressure drop evolved across the gradient, molecular diffusion and hence  
153 the column efficiency were not constant through the separation. Efficiency measurements were  
154 performed with compounds exhibiting  $k$  values around 3, using isocratic composition of either 5 %  
155 MeOH or 35 % MeOH and ranged from 17 000 to 9 000 plates, respectively. Hence the peak variance,  
156 resulting from the sum of column variance, instrumental variance and injection variance could not be  
157 compared from one test compound to another. The individual peak variances  $\sigma_{\text{MtBE}}^2$  were calculated  
158 from the reference chromatogram (Figure 1) and were in the range of 300-500  $\mu\text{L}^2$  (RSD < 10 %) for  
159 all test compounds, showing that the instrumental variance ( $\leq 37 \mu\text{L}^2$ ) was negligible under these  
160 conditions.

### 162 **3.1 Adsorption of the injection solvent**

163 Several SFC studies demonstrated that common polar solvents can exhibit retention on polar  
164 stationary phases [21, 22]. Detecting at 200 nm so that the MeOH co-solvent exhibited a significant  
165 absorbance, it was possible to follow the system peaks due to the elution of solvent molecules.

166 According to the displacement method [23, 24], the injection of a retained solvent produces two zones:  
167 the elution zone containing the injected molecules, called “tracer peak” that reflects the retention of the  
168 injected molecules, and the displaced elution zone called the “perturbation peak”. The injection of pure  
169 MtBE and pure ACN conducted to a single large negative perturbation peak around 0.6 min, while the  
170 injection of pure MeOH led to a right angled-triangular perturbation peak, suggesting that MeOH  
171 molecules are adsorbed on the stationary phase (Figure 2a). This MeOH adsorption on SFC  
172 stationary phases has already been evidenced [22]. The injection of pure ACN provided the exact  
173 same elution profile as the injection of MtBE, suggesting that ACN is not retained on the stationary  
174 phase. When injecting ACN/water mixtures (Figure 2b), the size and shape of this perturbation peak  
175 were not significantly affected by the amount of water. When injecting MeOH/water mixtures (Figure  
176 2c), the injected MeOH molecules eluted in the perturbation zone. Increasing the amount of injected  
177 MeOH increased the level of UV absorbance in this zone. This suggests that the co-solvent deficiency  
178 generated by the injection of ACN/water or MeOH/water migrates at the speed of the MeOH co-  
179 solvent, as expected [24].

180  
181 By injecting increasing amounts of water, it was also possible to observe a negative peak  
182 corresponding to the tracer peak of water, eluting later in the gradient. Figure 2d shows a right  
183 angled-triangular shape peak, which area increased with the injected amount of water. Using first-  
184 order moment [25], the retention time of this skewed peak was deduced at 2.00 min corresponding to  
185 a composition at elution of 13.7 % MeOH co-solvent, proving the large retention of water molecules on  
186 DEA stationary phase. Injecting water/ACN mixtures provided a tracer peak with the same retention  
187 time and shape, but slightly lower intensity. It is to be noted that during the course of these  
188 experiments using 5  $\mu$ L sample volume, no difference could be observed on the pressure trace that  
189 was highly repeatable whatever the diluent.

190  
191 Hence, when injecting samples in hydro-organic phases, both water and methanol molecules from the  
192 diluent competed with the analytes for the access to the stationary phase, while ACN molecules had  
193 no stationary phase interaction. Hence ACN/water diluents were expected to be less prone to  
194 generate injection effects than MeOH/water diluents.

195

### 196 **3.2 Influence of the diluent composition on peak broadening**

197 Studies on the effect of injection diluents on chromatographic performances have been performed by  
198 monitoring column efficiency [11, 22] or peak shapes [1]. However, the first is only applicable on  
199 isocratic separation while the latter may not properly reflect focusing/broadening phenomenon. As  
200 mentioned before [7], a slight retention shift occurred when increasing the water content in the diluent.

201 The contribution of the composition of the injection solvent to the process of peak broadening can be  
202 monitored as the relative variation of peak variance as compared to a similar injection with the sample  
203 diluted in MtBE. To more quantitatively describe the effect of the injection solvent on band broadening,  
204 the variance generated by the hydro-organic diluent  $\sigma_{diluent}^2$  was normalized in regards to the observed  
205 variance of the same peak when using MtBE as injection solvent  $\sigma_{MtBE}^2$ .

206 Figure 3 exhibits the influence of water content in the diluent on the peak broadening. The first  
207 observation was that injecting in pure ACN diluent (grey marks) resulted in a larger peak variance for  
208 early eluting peaks, as compared to MtBE diluent and as discussed in section 3.1, and had no effect  
209 on late-eluting peaks, as expected from a strong solvent effect. On the contrary, when the diluent  
210 contained water, the first eluting peaks, with composition at elution lower than 10 %, exhibited a clear  
211 compression, i.e. their variance when injected in hydro-organic solvent was lower than when injected  
212 in MtBE. For these compounds, the presence of water in the diluent had a clear beneficial effect.  
213 Compounds eluting later than the water plug, i.e. with composition at elution higher than 15 % MeOH,  
214 encountered a broadening effect. These observations are typical from displacement and tag-along  
215 effects when a column is overloaded, here with water molecules. This effect is well documented in  
216 preparative liquid chromatography, where the retention of major solutes affects the peak shape of  
217 minor solutes [26].

218  
219 In analytical SFC, Redei et al. [22] demonstrated that the retention of methanol diluent on an  
220 alkylamine column using neat CO<sub>2</sub> as mobile phase conducted to a focusing effect on low retained  
221 alkylbenzenes, a broadening effect on alkylbenzenes that were more retained than methanol and that  
222 alkylbenzenes that were greatly retained were unaffected by the presence of the diluent. Here we  
223 confirmed that the retention of water diluent on the diethylamine stationary phase conducted to a  
224 compression of peaks eluting at the initial composition of 5 % MeOH (compounds N1-N3), as soon as  
225 10 % water were added to the sample (Figure S1). The compression effect was related to the amount  
226 of water. Furthermore, when applying a gradient elution, this compression effect lasted as the amount  
227 of co-solvent increased. As shown in Figure 3, the extent of compression was directly linked to the  
228 retention of the analyte related to the water retention. The closer the analyte to the water molecules  
229 was located, the more compressed the peak was. This compression effect was also related to the  
230 amount of water that was injected alongside the low-retained analyte, down to a decrease in peak  
231 variance of 40 % when injecting in 90 % water.

232 On the other hand, the tag-along effect that broadened late-eluting peaks seemed to affect more  
233 significantly peaks with composition at elution over 30 % co-solvent, with variances reaching + 80 %,   
234 whereas for the test compound eluting at a composition of 18 % co-solvent, variance increased only  
235 by + 20 %.

236  
237 The displacement/tag-along effect is generated by retained molecules that interfere with the retention  
238 of analytes. As MeOH was proved to be retained on the SFC column, the dilution of the analytes in a  
239 MeOH/water phase had a different impact as when ACN/water was the diluent. For low-retained  
240 compounds diluted in over 80 % MeOH, a strong solvent effect was present, due to the competition  
241 with the MeOH molecules from the diluent (Figure S2a, black marks) and the compression usually  
242 generated by water (Figure S2a, ACN/water diluents, white marks) was annihilated by using MeOH as

243 part of the diluent. The broadening observed for peaks eluting before water, when diluent was 10/90  
244 MeOH/water, remains unexplained so far. Because MeOH exhibited a lower retention than water  
245 molecules, analyte peaks eluting after water underwent no competition with MeOH diluent molecules  
246 and hence their broadening was not significantly affected by the nature of the organic diluent (Figure  
247 S2b).

248

### 249 **3.3 Analyte position relative to water peak**

250 Since the water plug is beneficial for the analytes that migrate faster than water molecules, it may be  
251 tempting to modify the chromatographic conditions so that the retention of analytes becomes lower  
252 than that of the water. However, the retention of polar compounds in SFC usually follows the same  
253 trend and it was necessary to find a stationary phase for which the water retention trend ( $\ln k$  vs. co-  
254 solvent) intersects with test compounds. Isocratic experiments were performed at co-solvent  
255 volumetric fractions ranging from 2 to 40 %, injecting test compounds N6-N9 surrounding the water  
256 peak to determine their retention on DEA, diol and HILIC stationary phases (Figure S3). Models  
257 expressed as volumetric fractions are easier to use but they are valid only for given operating  
258 conditions, here 40 °C, 140 bars at BPR. Any transfer of models would require translation of  
259 volumetric fraction into mass fraction of co-solvent [20]. The retention data were fitting a HILIC mixed-  
260 mode model for the three columns (Figure S3). The position of test compounds relative to water  
261 elution could be switched on HILIC column by changing the gradient slope. At a normalized gradient  
262 slope of 2 % (Figure 4a), N9 eluted after water ( $C_e$  12.7 % MeOH vs. 9.3 % MeOH, respectively,  
263 calculated using first-order moment), whereas at 30 % normalized gradient slope (Figure 4b), N9  
264 eluted before water (27.3 % and  $C_e$  31.1 % MeOH, respectively). The faster elution resulted in an  
265 overall peak sharpening (Figure 4) as also observed in LC. For example, for N9 diluted in MtBE, the  
266 peak variance decreased from 600  $\mu\text{L}^2$  to 20  $\mu\text{L}^2$  for 2 % and 30% normalized gradient slopes,  
267 respectively. The effect of water in the diluent was hence normalized for each gradient slope to the  
268 variance when the diluent was MtBE. The change of position relative to the water peak confirmed the  
269 test compound was compressed if eluting before water molecules, as shown in Figure 4a and  
270 broadened if eluting after (figure 4b), with the extent of the phenomenon related to the water content in  
271 the diluent.

272

### 273 **3.4 Influence of the co-solvent nature**

274 Method development in SFC may require the use of different co-solvents to easily tune the separation.  
275 Methanol and acetonitrile are the most used co-solvents but mixture of both or ethanol are now  
276 gaining attention. As opposed to mobile phase components in LC, SFC co-solvent molecules are  
277 known to be prone to interaction with the stationary phase [21, 27]. The impact of the co-solvent  
278 nature was studied by comparing variances using MeOH, ACN, mixture of MeOH/ACN 50/50 and  
279 EtOH as co-solvent. Changing co-solvents did not affect the retention order of test compounds (Table  
280 S1) as polar molecules showed quite similar retention trends in SFC. Solutes injected in MtBE diluent  
281 were found to exhibit higher peak variance when the co-solvent was aprotic (ACN) than when it was  
282 protic (MeOH or EtOH) (Figure S4a). When the sample was diluted in a water-containing diluent, the  
283 trend in variance change was the same as described before, whatever the co-solvent. Solutes that



284 were less retained than water were subjected to two mechanisms: competition with the water diluent  
285 leading to peak compression, and competition with the co-solvent molecules to access the stationary  
286 phase. For a test compound eluting before water (white marks on Figure 5), it is clear that the  
287 competition from alcohol co-solvents (Figures 5a and 5b) was beneficial and the compression  
288 increased for peaks closer to water (here, N7). On the contrary, the injection of a water/ACN diluent in  
289 an aprotic co-solvent such as ACN (Figure 5c) led to broadening when the content of water was low,  
290 and to compression when the content of water in the diluent was elevated.

291 More surprisingly, the use of a mixture of ACN/MeOH 50:50 as a co-solvent, which is expected to  
292 generate less competition as less MeOH molecules compete with analytes, was highly compatible with  
293 the injection of water/ACN diluents, helping for the compression of early-eluting analyte peaks such as  
294 N1. This result has to be mitigated by the fact that MeOH/ACN co-solvent generated much larger  
295 peaks than any other co-solvent when injecting samples in apolar diluents (Figure S4a).

296 Finally, because the retention of the studied co-solvent was always lower than water molecules,  
297 analyzing compounds with large retention (grey marks in Figure 5) diluted in hydro-organic phases  
298 was not affected by the nature of the co-solvent used. Interestingly, Figure 5b suggests that injecting  
299 in a water-based diluent led to better results than injecting in MtBE when using an EtOH co-solvent.

300

### 301 **3.5 Effect of additives in co-solvent**

302 In recent years, water has been introduced as an additive in the organic co-solvent to enhance the  
303 mobile phase polarity range [28]. This addition of water, up to 7-8 % with methanol, exhibits a great  
304 opportunity for the separation of more polar compounds [29]. Another benefit of adding water to the  
305 co-solvent is its impact on peak shapes. Khvalbota et al. [30] reported an improvement in efficiency for  
306 neutral compounds isocratically separated on a Fructoshell-N stationary phase, as long as they were  
307 more retained than water. Moreover, efficiency was improved for neutral compounds on a silica  
308 column, whatever their relative positive towards water.

309 Adding 2 % water in MeOH co-solvent had very little yet positive effects on the gradient separation of  
310 neutral test compounds on the DEA stationary phase. Retention was slightly reduced (Table S1).  
311 When injection was performed using MtBE, the peak variance was improved for all compounds by 10  
312 % - 20 % using water as an additive in co-solvent (Figure S4b). This behavior is similar to what was  
313 observed on the silica shell column by Khvaltova [30]. However, the beneficial effect of adding water to  
314 the co-solvent was reduced when the sample was also in an aqueous media. As can be seen in Figure  
315 6, when comparing the absolute peak variance obtained when using no additive (Figure 6a) or when  
316 using water as an additive (Figure 6b), the trend was very similar. Here again, the compounds eluting  
317 before the water molecules were compressed, but the influence of the water content in the diluent  
318 acted to a lesser extent, the peak variance being already influenced by the water adsorbed on the  
319 stationary phase prior to injection. In addition, the tag-along phenomenon was also reduced, with the  
320 peak variance increasing by 40 % over the range of diluent composition, compared to 70% when  
321 using no additive. This may be due to the fact that the competition between analytes and water for the  
322 stationary phase lasted all along the gradient run and not just in the water injection plug. Hence the  
323 presence of water in the co-solvent tended to level the effects of water in the diluent, whether  
324 beneficial or detrimental.

325

326 In order to introduce an additive that would efficiently compete with the water molecules from the  
327 injection solvent, formic acid (FA) was investigated. Anionic additives are often used to improve peak  
328 shape when using stationary phases with a basic character such as the Torus DEA [31]. Formic acid  
329 can be used in SFC as an alternative to TFA as column regeneration is faster [32]. Formic acid was  
330 more retained than water on DEA stationary phase, with a  $C_e$  of 23.5 % MeOH. A concentration of 0.1  
331 % FA in the methanol co-solvent did not affect the retention of neutral test compounds (Table S1).  
332 However, it broadened the peaks significantly for 7 out of 10 compounds using MtBE as diluent  
333 (Figure S4b). When comparing the absolute peak variances obtained when injecting in water-  
334 containing diluents, the addition of formic acid in the MeOH co-solvent improved the peak variances of  
335 retained compounds N8-N10 (Figure 6c), by a factor 30 % - 50 % compared to the use of pure MeOH  
336 as co-solvent, while it had a dramatic effect on less retained compounds N4-N7 with absolute peak  
337 variances increasing by a factor 3. Hence, formic acid as an additive to MeOH has to be avoided if  
338 MtBE is the sample diluent. Nonetheless it may be of interest for highly polar solutes diluted in  
339 ACN/water.

340

### 341 **3.6 Ionizable solutes**

342 The expansion of SFC applications towards more polar compounds such as metabolites, amino acids,  
343 nucleoside, peptides [2] pave the road towards the analysis of ionized molecules by LC x SFC. These  
344 highly polar analytes typically elute from LC in a great amount of water thus it seemed essential to  
345 check the behavior of ionized test compounds in this study.

346 West et al. stated using pH indicator that the apparent aqueous pH of carbon dioxide – methanol  
347 compositions should be around pH 5 with a decreased value when the proportion of methanol  
348 increased [33]. The selected acidic test compounds ( $pK_a$  around 4.5) were supposed to be partially  
349 ionized. Interestingly, the peak variance of acidic compounds was not influenced by the content of  
350 water in the diluent (Figure 7).

351 With composition at elution over 20 % MeOH, the selected acidic test compounds A1-A3 were highly  
352 retained. However, no peak broadening was observed on these negative analytes, whatever the  
353 content of water in the diluent while neutral compounds eluting at the same composition (N4 and N8)  
354 suffered an increase in peak width which extent was linked to the water content in the diluent, as  
355 previously discussed.

356 On the other hand, two basic test compounds B1 and B2 were analyzed, B1 with a lower retention  
357 than water, and B2 with a larger retention than water. Ammonium hydroxide was added to the co-  
358 solvent to improve peak symmetry [14]. Selected test compounds had both a  $pK_a$  at 9.4 and so the  
359 assumption can be made that they were fully protonated all along the gradient run. Unlike for other test  
360 compounds, MtBE as an injection solvent was found to provide symmetrical yet very wide peaks.  
361 Hence a mixture of ACN/water 90:10 was used as the injection solvent of reference for the calculation  
362 of variance change. The general trend for basic solutes followed what was observed for neutral  
363 solutes, with a peak compression for compounds eluting before the water peak and an increase in  
364 peak width for compounds more retained than water (Figure 7b). The compression on low-retained B1  
365 peak ranged between -5 % and - 20 % depending on the water content, which was very close to the  
366 value observed for the neutral test compound N4 eluting at the same composition. On the other hand,  
367 the selected retained basic compound B2 eluted at  $C_e$  15 % MeOH which was very close to the water

368 peak. The increase in peak width that B2 underwent was of a much larger extent than the one  
369 observed for the neutral test compound N8 eluting at its vicinity.

370  
371 While these results need to be confirmed with a much larger pool of ionizable compounds, it seems  
372 that in the case of our selected test compounds, negatively charged solutes and positively charged  
373 solutes exhibiting a lower retention than water molecules were not influenced by the water content in  
374 the injection solvent. On the contrary, the presence of water-rich solvent was detrimental for the  
375 positively-charged compounds with a retention close to water.

376  
377 Adding 2 % water to the co-solvent was positive for the peak shapes of basic compounds when the  
378 injection solvent was of low polarity such as MtBE, as previously stated by West and Lemasson [34],  
379 but it was found highly detrimental when injecting in a water-based phase (Figure S5a). Injecting water  
380 in a water-containing co-solvent led to the formation of a perturbation peak at 2.5 min and a tracer  
381 peak at 3.4 min, visible at 200 nm (Figure S5b). With water content as low as 10 % in the diluent, the  
382 peaks of basic compounds eluting before the perturbation peak were splitting towards higher retention.  
383 The peaks with higher retention kept symmetrical shape up to 30 % water in the diluent, then when  
384 increasing the amount of water in the diluent, the peaks also splitted towards higher retention. In  
385 comparison, acidic or neutral compounds never underwent any splitting in the same conditions.

386

### 387 **3.7 Increasing the injection volume**

388 Desfontaines et al. [1] stated that injection of samples with high content of water was possible for low  
389 injection volume ( $< 2 \mu\text{L}$ ) while the injection of  $10 \mu\text{L}$  (2 % column volume) conducted to a demixing  
390 when using an initial mobile phase containing only 2 % co-solvent (MeOH/water 98:2 + 0.1 %  
391 ammonium hydroxide). The solubility of water is indeed very low in supercritical  $\text{CO}_2$  ( $\sim 0.1\%$  w/w).  
392 Increasing the initial mobile phase composition to 5 % MeOH increased the solubility of water and  
393 during the course of our experiments, a volume of  $10 \mu\text{L}$  of a sample diluted in pure water could be  
394 injected on a column of similar geometry (100 x 3.0 mm,  $1.7 \mu\text{m}$ ) without demixing issue. Increasing  
395 the injection volume from  $5 \mu\text{L}$  to  $10 \mu\text{L}$  led to an expected peak broadening but the peaks remained  
396 symmetrical, and retention times and system pressure kept unchanged. The peak capacity when  
397 injecting in water-containing diluents remained above 75 % of the peak capacity observed when  
398 injecting  $10 \mu\text{L}$  sample in MtBE. Increasing the injection volume to  $20 \mu\text{L}$  (4 % column volume) led to  
399 two increases in the profile of the system pressure (Figure S6a). The first one occurred during the  
400 elution of MeOH molecules while the second one occurred during the elution of water molecules.  
401 Since both increases were proportional to the amount of water injected in the column, we suggest they  
402 were due to the local increase of viscosity generated by 1) the displaced MeOH molecules and 2) the  
403 water plug. Pressure values were back to normal as soon as water eluted out of the column. While  
404 peaks were broadening and splitting with an increase content of water in the diluent, injecting 90%  
405 water diluent led to a massively distorted broad peak for compounds eluting at the vicinity of water  
406 molecules (Figure 8). However, the system peak due to water was visible at the same time at it was  
407 when injecting  $5 \mu\text{L}$  (Figure S6b) and the UV signal was not disrupted, suggesting that water plug still  
408 eluted at the same velocity and demixing was not happening. A better understanding of water

409 interaction with stationary phase and solutes in SFC would be required before injecting such amount  
410 of water diluent.

411 On the other hand, neutral test compounds eluting at the end of the gradient, such as N10, exhibited  
412 fronting peaks while peaks from acidic test compounds with the same retention time remained  
413 symmetrical with no retention shift (Figure 8). Supposedly, ionic interactions with the stationary phase  
414 in SFC played a role in maintaining the peak symmetry for acidic test compounds in this study, but this  
415 point needs a deeper investigation with a larger set of ionizable compounds.

416

## 417 **4. Conclusion**

418 The composition of the sample diluent has a major role in the peak broadening in SFC. While previous  
419 papers highlighted the strong solvent effect due to polar solvents such as alcohols, this work focuses  
420 on the injection of water-based diluents. Peak broadening of 10 test compounds were compared when  
421 injected either in MtBE or in diluents containing up to 90 % water. Statements that water has a  
422 negative effect on peak shape when it is part of the diluent is only partly true. When injected  
423 simultaneously with neutral analytes, water plays a competing role for the SFC stationary phase,  
424 leading to a compression of peaks that elute before water, and a broadening of peaks that elute after  
425 water. The phenomenon is related to 1) the retention of analytes in regards to the retention of water  
426 and 2) the amount of water in the diluent. It has been confirmed on various stationary phases. Adding  
427 water or acidic additive to the co-solvent did not affect this process for neutral analytes. The presence  
428 of water along acidic analytes in the sample had no effect on their peak shapes, while for basic  
429 compounds, it led to dramatic peak deformation. Moreover it was possible to inject 10  $\mu\text{L}$  of samples in  
430 water-containing diluents (2 % column volume) without major peak capacity loss, while increasing the  
431 injection volume up to 20  $\mu\text{L}$  had negative consequences on peak shapes of neutral molecules. In the  
432 light of these results, the analysis of polar compounds diluted in hydro-organic mixtures, or the use of  
433 SFC as second dimension in a two-dimensional separation of neutral compounds could be considered  
434 without requiring sample water removal, providing that injection volume remained below 2 % of the  
435 column volume. Interestingly, acidic compounds can hold very large injection volumes with water-rich  
436 diluents, while the analysis of basic compounds seems problematic even at very small injection  
437 volume. While this study highlighted clear trends for neutral compounds, a deeper investigation will be  
438 required for ionizable compounds.

439

## 440 **5. Acknowledgments**

441 The authors are deeply grateful to Agilent Technologies for the loan of the Infinity I fixed-loop injection  
442 module and especially Audrey Menet for her technical advices. Marion Bulet-Parendel is  
443 acknowledged for preliminary results.

444

## 445 **6. References**

- 447 [1] V. Desfontaine, A. Tarafder, J. Hill, J. Fairchild, A. Grand-Guillaume Perrenoud, J.-L. Veuthey, D.  
448 Guillaume, A systematic investigation of sample diluents in modern supercritical fluid chromatography,  
449 *Journal of Chromatography A* 1511 (2017) 122-131 <https://doi.org/10.1016/j.chroma.2017.06.075>.
- 450 [2] G.L. Losacco, J.-L. Veuthey, D. Guillaume, Metamorphosis of supercritical fluid chromatography: A  
451 viable tool for the analysis of polar compounds?, *TrAC Trends in Analytical Chemistry* 141 (2021)  
452 116304 <https://doi.org/10.1016/j.trac.2021.116304>.
- 453 [3] M. Burlet-Parendel, K. Faure, Opportunities and challenges of liquid chromatography coupled to  
454 supercritical fluid chromatography, *TrAC Trends in Analytical Chemistry* 144 (2021) 116422  
455 <https://doi.org/10.1016/j.trac.2021.116422>.
- 456 [4] A.S. Kaplitz, M.E. Mostafa, S.A. Calvez, J.L. Edwards, J.P. Grinias, Two-dimensional separation  
457 techniques using supercritical fluid chromatography, *Journal of Separation Science* 44 (2021) 426-437  
458 <https://doi.org/10.1002/jssc.202000823>.
- 459 [5] M. Enmark, D. Åsberg, A. Shalliker, J. Samuelsson, T. Fornstedt, A closer study of peak distortions  
460 in supercritical fluid chromatography as generated by the injection, *Journal of Chromatography A* 1400  
461 (2015) 131-139 <https://doi.org/10.1016/j.chroma.2015.04.059>.
- 462 [6] K. Vanderlinden, G. Desmet, K. Broeckhoven, Effect of the feed injection method on band  
463 broadening in analytical supercritical fluid chromatography, *Journal of Chromatography A* 1630 (2020)  
464 461525 <https://doi.org/10.1016/j.chroma.2020.461525>.
- 465 [7] M. Sarrut, A. Corgier, G. Cretier, A. Le Masle, S. Dubant, S. Heinisch, Potential and limitations of  
466 on-line comprehensive reversed phase liquid chromatography x supercritical fluid chromatography for  
467 the separation of neutral compounds: An approach to separate an aqueous extract of bio-oil, *Journal*  
468 *of Chromatography A* 1402 (2015) 124-133 [10.1016/j.chroma.2015.05.005](https://doi.org/10.1016/j.chroma.2015.05.005).
- 469 [8] M. Sun, M. Sandahl, C. Turner, Comprehensive on-line two-dimensional liquid  
470 chromatography x supercritical fluid chromatography with trapping column-assisted modulation for  
471 depolymerised lignin analysis, *Journal of Chromatography A* 1541 (2018) 21-30  
472 <https://doi.org/10.1016/j.chroma.2018.02.008>.
- 473 [9] C.J. Venkatramani, M. Al-Sayah, G. Li, M. Goel, J. Girotti, L. Zang, L. Wigman, P. Yehl, N.  
474 Chetwyn, Simultaneous achiral-chiral analysis of pharmaceutical compounds using two-dimensional  
475 reversed phase liquid chromatography-supercritical fluid chromatography, *Talanta* 148 (2016) 548-555  
476 <https://doi.org/10.1016/j.talanta.2015.10.054>.
- 477 [10] M. Goel, E. Larson, C.J. Venkatramani, M.A. Al-Sayah, Optimization of a two-dimensional liquid  
478 chromatography-supercritical fluid chromatography-mass spectrometry (2D-LC-SFC-MS) system to  
479 assess "in-vivo" inter-conversion of chiral drug molecules, *Journal of Chromatography B* 1084 (2018)  
480 89-95 <https://doi.org/10.1016/j.jchromb.2018.03.029>.
- 481 [11] R. De Pauw, K. Shoykhet, G. Desmet, K. Broeckhoven, Understanding and diminishing the extra-  
482 column band broadening effects in supercritical fluid chromatography, *Journal of Chromatography A*  
483 1403 (2015) 132-137 <https://doi.org/10.1016/j.chroma.2015.05.017>.
- 484 [12] M. Enmark, E. Glenne, M. Leško, A. Langborg Weinmann, T. Leek, K. Kaczmarski, M. Klarqvist,  
485 J. Samuelsson, T. Fornstedt, Investigation of robustness for supercritical fluid chromatography  
486 separation of peptides: Isocratic vs gradient mode, *Journal of Chromatography A* 1568 (2018) 177-187  
487 <https://doi.org/10.1016/j.chroma.2018.07.029>.
- 488 [13] C. West, Current trends in supercritical fluid chromatography, *Analytical and Bioanalytical*  
489 *Chemistry* 410(25) (2018) 6441-6457 [10.1007/s00216-018-1267-4](https://doi.org/10.1007/s00216-018-1267-4).
- 490 [14] A. Grand-Guillaume Perrenoud, J.-L. Veuthey, D. Guillaume, Comparison of ultra-high  
491 performance supercritical fluid chromatography and ultra-high performance liquid chromatography for  
492 the analysis of pharmaceutical compounds, *Journal of Chromatography A* 1266 (2012) 158-167  
493 <https://doi.org/10.1016/j.chroma.2012.10.005>.
- 494 [15] M.A. Khalikova, E. Lesellier, E. Chapuzet, D. Šatinský, C. West, Development and validation of  
495 ultra-high performance supercritical fluid chromatography method for quantitative determination of nine  
496 sunscreens in cosmetic samples, *Analytica Chimica Acta* 1034 (2018) 184-194  
497 <https://doi.org/10.1016/j.aca.2018.06.013>.
- 498 [16] Y. Huang, T. Zhang, Y. Zhao, H. Zhou, G. Tang, M. Fillet, J. Crommen, Z. Jiang, Simultaneous  
499 analysis of nucleobases, nucleosides and ginsenosides in ginseng extracts using supercritical fluid  
500 chromatography coupled with single quadrupole mass spectrometry, *Journal of Pharmaceutical and*  
501 *Biomedical Analysis* 144 (2017) 213-219 <https://doi.org/10.1016/j.jpba.2017.03.059>.
- 502 [17] R. De Pauw, K. Shoykhet, G. Desmet, K. Broeckhoven, Effect of reference conditions on flow  
503 rate, modifier fraction and retention in supercritical fluid chromatography, *Journal of Chromatography*  
504 *A* 1459 (2016) 129-135 <https://doi.org/10.1016/j.chroma.2016.06.040>.
- 505 [18] G. Guiochon, A. Tarafder, Fundamental challenges and opportunities for preparative supercritical  
506 fluid chromatography, *Journal of Chromatography A* 1218(8) (2011) 1037-1114  
507 <https://doi.org/10.1016/j.chroma.2010.12.047>.

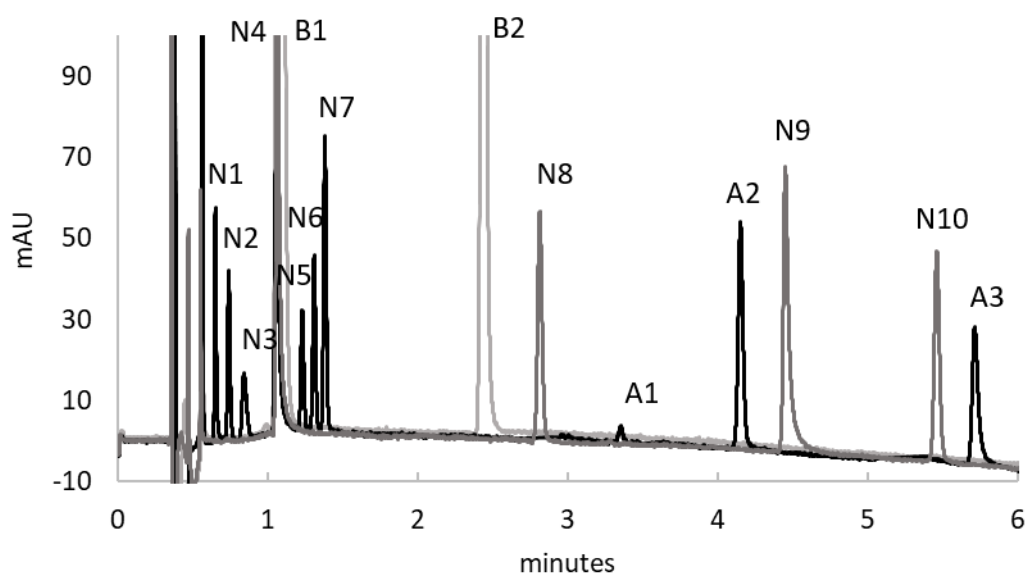
508 [19] E. Glenne, H. Leek, M. Klarqvist, J. Samuelsson, T. Fornstedt, Systematic investigations of peak  
509 deformations due to co-solvent adsorption in preparative supercritical fluid chromatography, *Journal of*  
510 *Chromatography A* 1496 (2017) 141-149 <https://doi.org/10.1016/j.chroma.2017.03.053>.  
511 [20] M. Enmark, J. Samuelsson, T. Fornstedt, A Retention-Matching Strategy for Method Transfer in  
512 Supercritical Fluid Chromatography: Introducing the Isomolar Plot Approach, *Analytical Chemistry*  
513 93(16) (2021) 6385-6393 10.1021/acs.analchem.0c05142.  
514 [21] E. Glenne, K. Öhlén, H. Leek, M. Klarqvist, J. Samuelsson, T. Fornstedt, A closer study of  
515 methanol adsorption and its impact on solute retentions in supercritical fluid chromatography, *Journal*  
516 *of Chromatography A* 1442 (2016) 129-139 <https://doi.org/10.1016/j.chroma.2016.03.006>.  
517 [22] C. Rédei, A. Felinger, Modeling the competitive adsorption of sample solvent and solute in  
518 supercritical fluid chromatography, *Journal of Chromatography A* 1603 (2019) 348-354  
519 <https://doi.org/10.1016/j.chroma.2019.05.045>.  
520 [23] P. Forssén, J. Lindholm, T. Fornstedt, Theoretical and experimental study of binary perturbation  
521 peaks with focus on peculiar retention behaviour and vanishing peaks in chiral liquid chromatography,  
522 *Journal of Chromatography A* 991(1) (2003) 31-45 [https://doi.org/10.1016/S0021-9673\(03\)00213-9](https://doi.org/10.1016/S0021-9673(03)00213-9).  
523 [24] T. Fornstedt, P. Forssén, D. Westerlund, System peaks and their impact in liquid chromatography,  
524 *TrAC Trends in Analytical Chemistry* 81 (2016) 42-50 <https://doi.org/10.1016/j.trac.2016.01.008>.  
525 [25] J.P. Foley, J.G. Dorsey, Equations for Calculation of Chromatographic Figures of Merit for Ideal  
526 and Skewed Peaks, *Anal. Chem.* 83(55) (1983) 730-737  
527 [26] S. Golshan-Shirazi, G. Guiochon, Theoretical explanation of the displacement and tag-along  
528 effects, *Chromatographia* 30(11) (1990) 613-617 10.1007/BF02269733.  
529 [27] P. Vajda, G. Guiochon, Modifier adsorption in supercritical fluid chromatography onto silica  
530 surface, *Journal of Chromatography A* 1305 (2013) 293-299  
531 <https://doi.org/10.1016/j.chroma.2013.06.075>.  
532 [28] D. Roy, A. Tarafder, L. Miller, Effect of water addition to super/sub-critical fluid mobile-phases for  
533 achiral and chiral separations, *TrAC Trends in Analytical Chemistry* 145 (2021) 116464  
534 <https://doi.org/10.1016/j.trac.2021.116464>.  
535 [29] G.L. Losacco, O. Ismail, J. Pezzatti, V. González-Ruiz, J. Boccard, S. Rudaz, J.-L. Veuthey, D.  
536 Guillaume, Applicability of Supercritical fluid chromatography–Mass spectrometry to metabolomics. II–  
537 Assessment of a comprehensive library of metabolites and evaluation of biological matrices, *Journal of*  
538 *Chromatography A* 1620 (2020) 461021 <https://doi.org/10.1016/j.chroma.2020.461021>.  
539 [30] L. Khvalbota, D. Roy, M.F. Wahab, S.K. Firooz, A. Machyňáková, I. Špánik, D.W. Armstrong,  
540 Enhancing supercritical fluid chromatographic efficiency: Predicting effects of small aqueous additives,  
541 *Analytica Chimica Acta* 1120 (2020) 75-84 <https://doi.org/10.1016/j.aca.2020.04.065>.  
542 [31] G.L. Losacco, J.O. DaSilva, J. Liu, E.L. Regalado, J.-L. Veuthey, D. Guillaume, Expanding the  
543 range of sub/supercritical fluid chromatography: Advantageous use of methanesulfonic acid in water-  
544 rich modifiers for peptide analysis, *Journal of Chromatography A* 1642 (2021) 462048  
545 <https://doi.org/10.1016/j.chroma.2021.462048>.  
546 [32] C. Brunelli, Y. Zhao, M.-H. Brown, P. Sandra, Pharmaceutical analysis by supercritical fluid  
547 chromatography: Optimization of the mobile phase composition on a 2-ethylpyridine column, *Journal*  
548 *of Separation Science* 31(8) (2008) 1299-1306 <https://doi.org/10.1002/jssc.200700555>.  
549 [33] C. West, J. Melin, H. Ansouri, M. Mengue Metogo, Unravelling the effects of mobile phase  
550 additives in supercritical fluid chromatography. Part I: Polarity and acidity of the mobile phase, *Journal*  
551 *of Chromatography A* 1492 (2017) 136-143 <https://doi.org/10.1016/j.chroma.2017.02.066>.  
552 [34] C. West, E. Lemasson, Unravelling the effects of mobile phase additives in supercritical fluid  
553 chromatography—Part II: Adsorption on the stationary phase, *Journal of Chromatography A* 1593  
554 (2019) 135-146 <https://doi.org/10.1016/j.chroma.2019.02.002>.  
555

556  
557  
558  
559  
560

Table 1: Selected **test compounds** and associated retention time and composition at elution **using DEA column**. MeOH as co-solvent for neutral and acidic compounds, **MeOH + 2 % water + 20 mM ammonium hydroxide for basic compounds**.

	Probe number	log P	tr (min)	Ce (%)	
Neutral	eugenol	N1	2.223	0.65	5.0
	2.4.6 trimethylphenol	N2	1.7	0.74	5.0
	1-indanol	N3	1.518	0.84	5.0
	apocynin	N4	0.77	1.05	6.3
	o-cresol	N5	1.95	1.23	7.5
	m-cresol	N6	1.96	1.31	8.0
	phenol	N7	1.46	1.38	8.5
	4-hydroxybenzyl alcohol	N8	-0.121	2.81	17.9
	naringenin	N9	0.79	4.45	28.7
	arbutin	N10	-0.652	5.45	35.3
Acidic	acrylic acid	A1	0.35	3.35	21.4
	trans cinnamic acid	A2	1.887	4.15	26.7
	ferulic acid	A3	0.78	5.71	37.0
Basic	imipramine	B1	3.112	1.08	6.4
	propranolol	B2	2.535	2.44	15.4

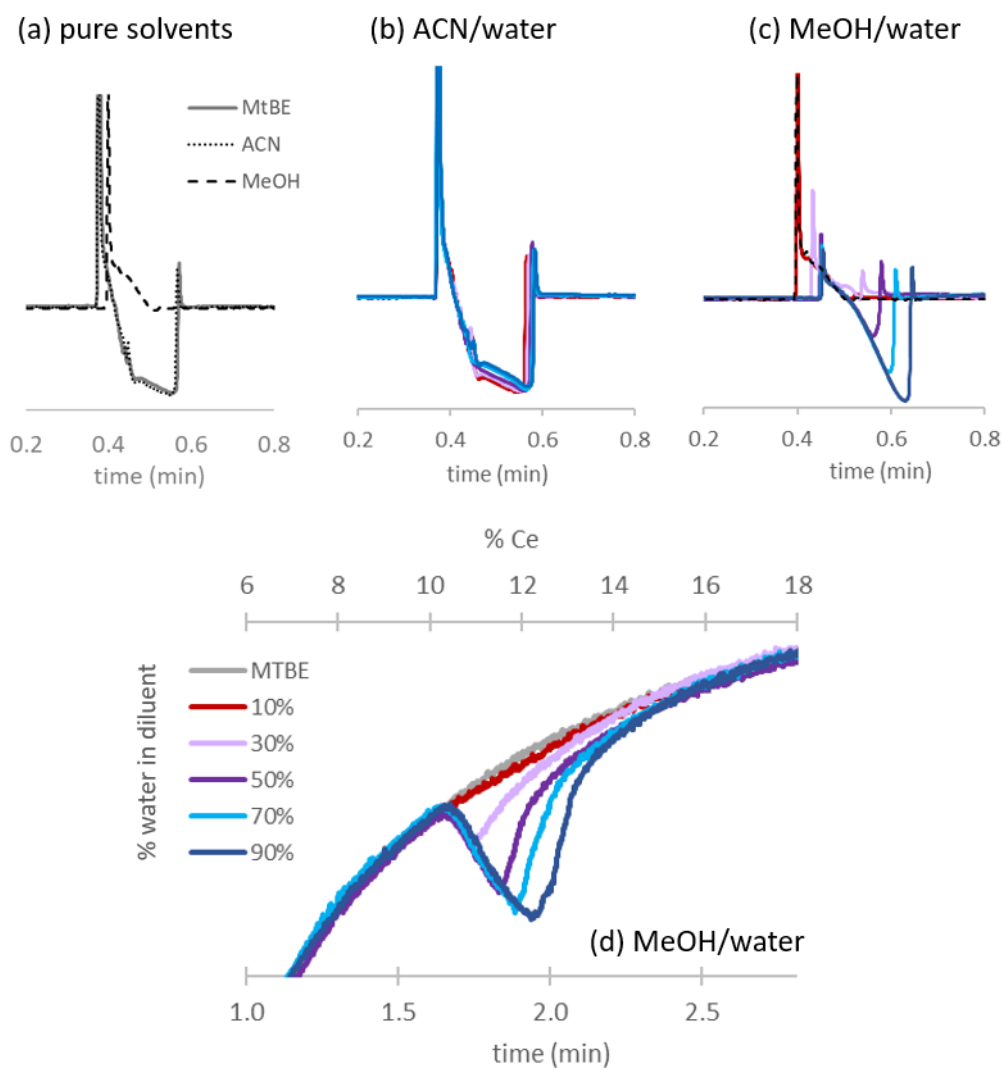
561  
562  
563



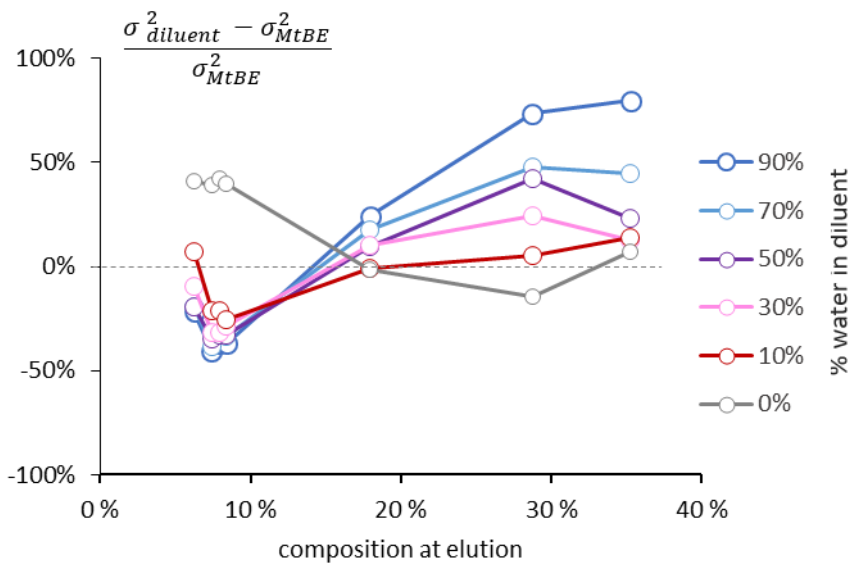
564  
 565  
 566  
 567  
 568  
 569  
 570

Figure 1: Separation of the 15 test compounds. Column DEA. Co-solvent MeOH for neutral and acidic compounds (N1-N10; A1-A3) and co-solvent MeOH + 2 % water + 20 mM ammonium hydroxide for basic compounds (B1-B2). Injection 5  $\mu$ L in MtBE diluent. Detection 220 nm. Test compounds description: refer to table 1.



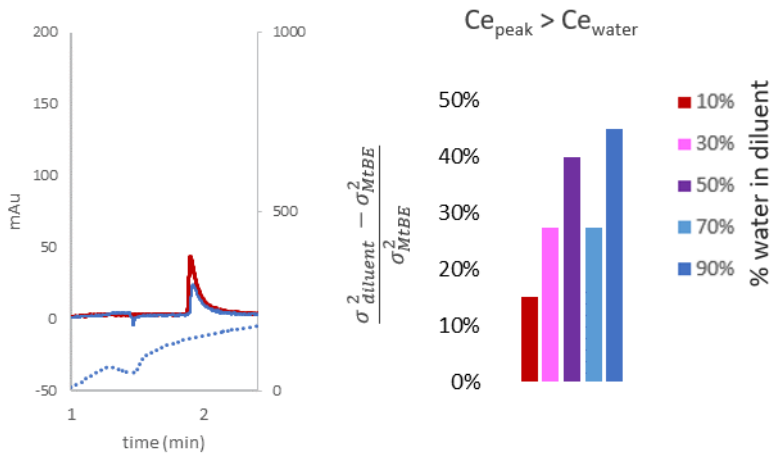


571  
 572  
 573 Figure 2: Chromatograms corresponding to the injection of (a) pure diluents: MtBE (grey line), ACN  
 574 (dotted line) and MeOH (dashed line), (b) ACN/water mixtures and (c, d) MeOH/water mixtures. The  
 575 colored lines correspond to increasing amounts of water in diluent, from 10 % (red line) to 90 % (blue  
 576 line). Column DEA. Co-solvent MeOH. Injection volume 5  $\mu$ L. Detection at 200 nm.  
 577

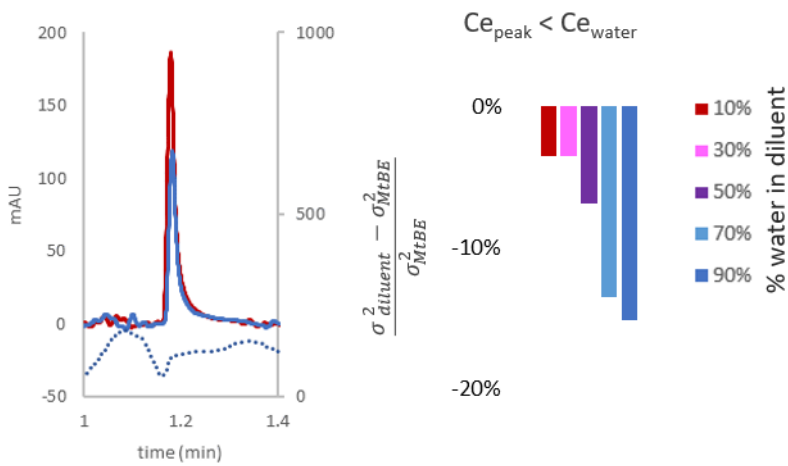


578  
 579 Figure 3: Diluent effect reported as change in peak variance vs. the composition at elution of neutral  
 580 test compounds, for various percentages of water in the ACN: water diluent. Reference variance from  
 581 the injection of test compounds using MtBE as diluent, with conditions as in Figure 1.  
 582  
 583

(a) normalized gradient slope 2 %



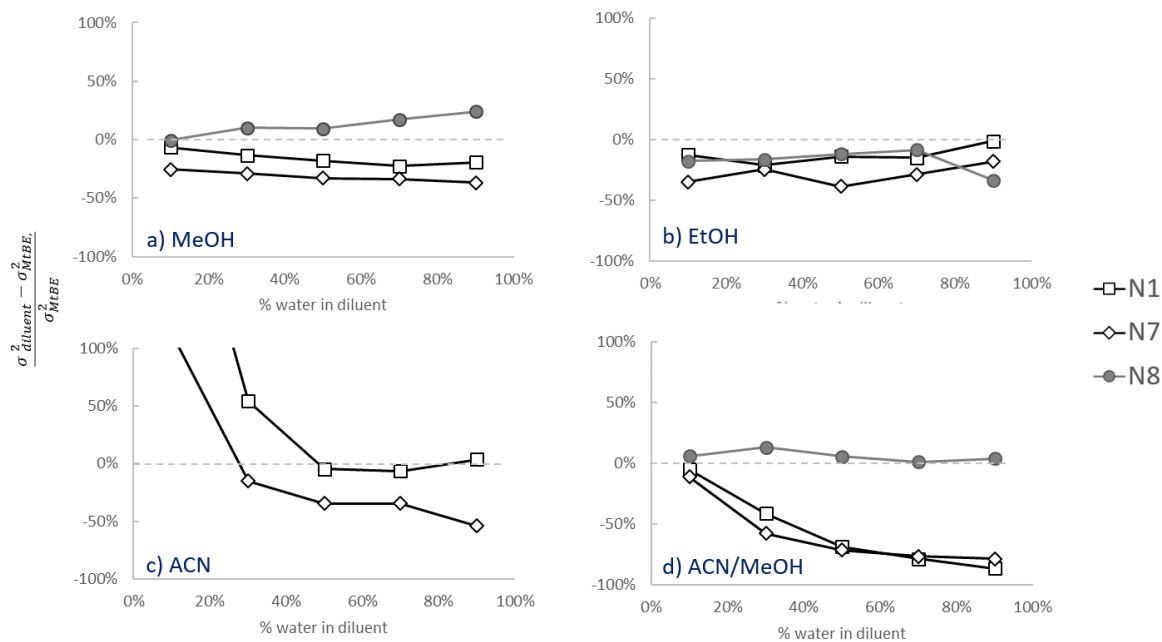
(b) normalized gradient slope 30 %



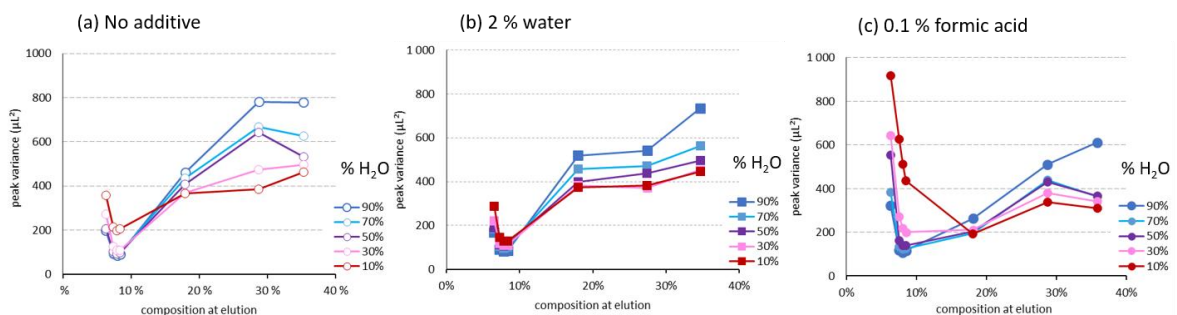
584

585 Figure 4: Chromatograms of N9 (plain line, 220 nm) and water (dashed line, 200 nm) and associated  
 586 injection solvent effects, for a) a normalized gradient slope of 2 % and b) a normalized gradient slope  
 587 of 30 %. HILIC column, gradient 5 % to 40 % MeOH.

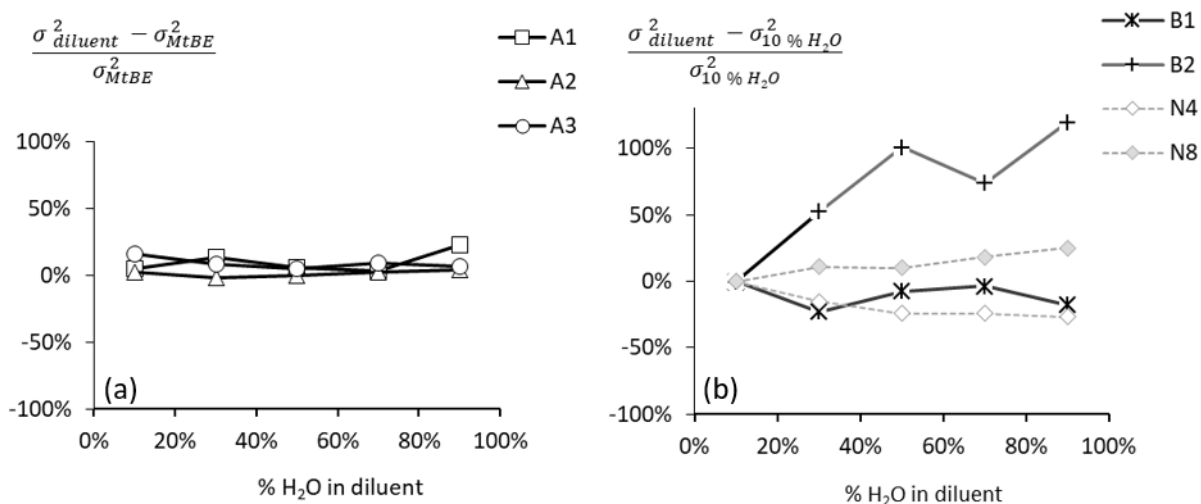
588



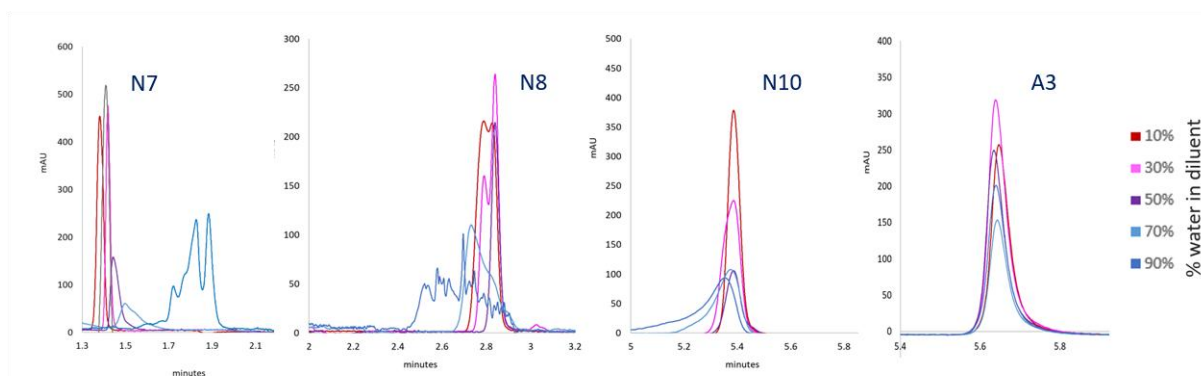
589  
 590 Figure 5: Influence of the co-solvent on the change in peak variance vs. the content of water in the  
 591 ACN/H<sub>2</sub>O diluent, for co-solvent (a) MeOH, (b) ACN, (c) EtOH and (d) MeOH/ACN 50/50. Compounds  
 592 N1-N7 (black marks) elute before water, N8 (grey marks) after water. Please refer to Table S1 for the  
 593 values of composition at elution in the different co-solvents.  
 594



595  
 596 Figure 6: Effect of additives in modifier on the peak variance for various water content in the  
 597 ACN/water diluent. Mobile phase CO<sub>2</sub> with the co-solvent (a) MeOH, (b) MeOH +2 % v/v water and (c)  
 598 MeOH + 0.1 % w/w formic acid  
 599



600  
 601 Figure 7: Diluent effect reported as change in peak variance vs. the content of water in the diluent. (a)  
 602 acidic test compounds A1-A3, with MtBE diluent as reference and (b) basic test compounds B1-B2  
 603 with ACN/water 90:10 diluent as reference. The dashed lines represent test compounds N4 (white  
 604 diamond) and N8 (grey diamond).  
 605



606  
 607 Figure 8. Chromatograms of three neutral probes and one acidic probe. Injection 20  $\mu$ L. Column DEA.  
 608 Co-solvent MeOH. UV detection 220 nm. Other conditions as stated in the text.  
 609

610  
611  
612  
613  
614  
615  
616  
617  
618  
619  
620  
621  
622  
623  
624  
625  
626  
627  
628  
629  
630  
631  
632  
633  
634  
635  
636  
637  
638  
639  
640  
641  
642  
643  
644  
645  
646  
647  
648  
649  
650

## Supplementary material

### Effect of the injection of water-containing diluents on band broadening in analytical supercritical fluid chromatography

Magali Batteau<sup>1</sup>, Karine Faure<sup>1</sup>

<sup>1</sup>Université de Lyon, CNRS, Université Claude Bernard Lyon 1, Institut des Sciences Analytiques, UMR 5280, 5 rue de la Doua, F-69100 VILLEURBANNE, France

\*Corresponding author: [karine.faure@isa-lyon.fr](mailto:karine.faure@isa-lyon.fr)

#### List of supplementary material

Figure S1: Change in peak variance for peaks N1-N3 eluting at initial mobile phase composition, for various percentages of water in the ACN/water diluent. Column DEA, co-solvent MeOH.

Figure S2: Injection solvent effect reported as change in peak variance for (a) N6 and (b) N10 vs. the content of water in the diluent, the remaining solvent being acetonitrile (white marks) or methanol (black marks).

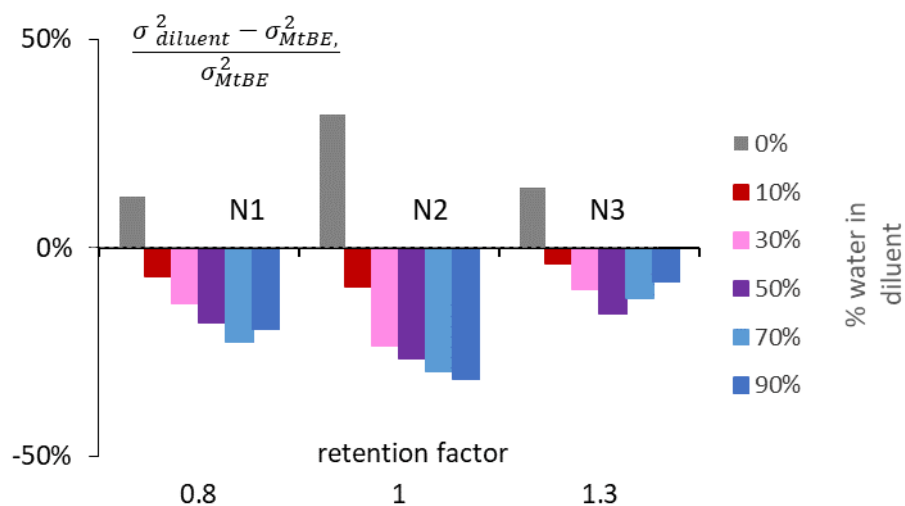
Figure S3: Retention relationships of water and four surrounding probes N6-N9.  $\ln k$  as a function of the MeOH content in mobile phase. Circles are experimental measurements based on isocratic runs. Plain lines are the associated prediction using mixed-mode model. Below are the associated prediction errors of three models. Percentage errors defined as  $(k_{\text{predicted}} - k_{\text{exp}})/k_{\text{exp}}$ . Columns (a) Torus DEA, (b) Torus diol and (c) BEH HILIC.

Figure S4: Peak variance of the neutral test compounds, using MtBE as diluent, (a) for various organic co-solvents and (b) using MeOH with additives, i.e. 2 % water or 0.1 % formic acid additives as co-solvent. Compounds N8-N10 were not eluting during the gradient when using ACN as co-solvent.

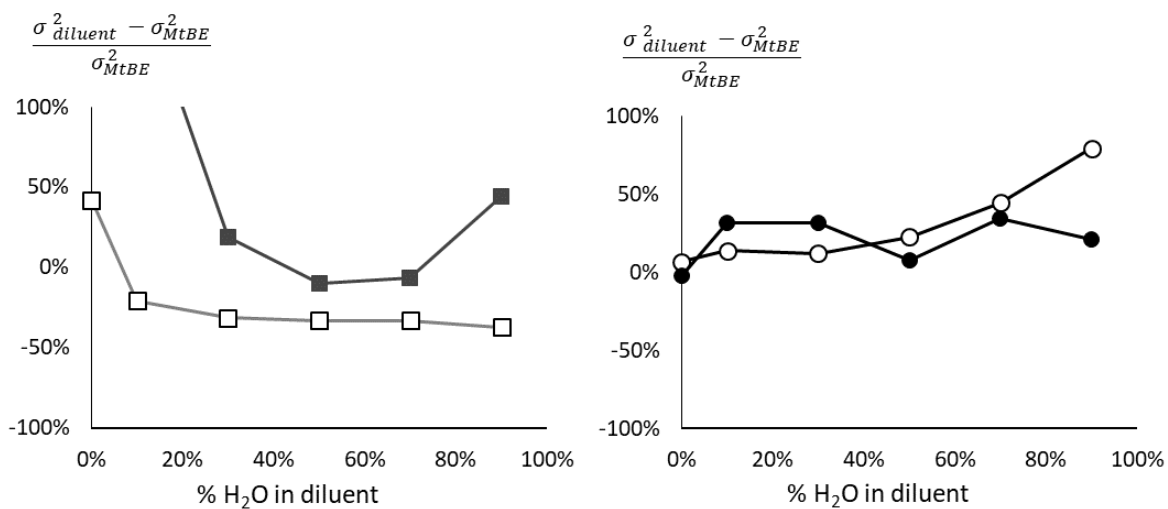
Figure S5: (a) Chromatograms of two basic probes injected in ACN/water diluent with increasing content of water. UV detection 220 nm. (b) UV trace of pure water. UV detection 200 nm. Column DEA. Co-solvent MeOH + 2 % water + 20 mM ammonium hydroxide.

Figure S6: a) SFC inlet pressure when injecting 20  $\mu\text{L}$  ACN/water with increasing content of water and b) System peaks recorded at 200 nm, when injecting 5  $\mu\text{L}$  and 20  $\mu\text{L}$  pure water. Column DEA. Co-solvent MeOH. Other conditions stated in text.

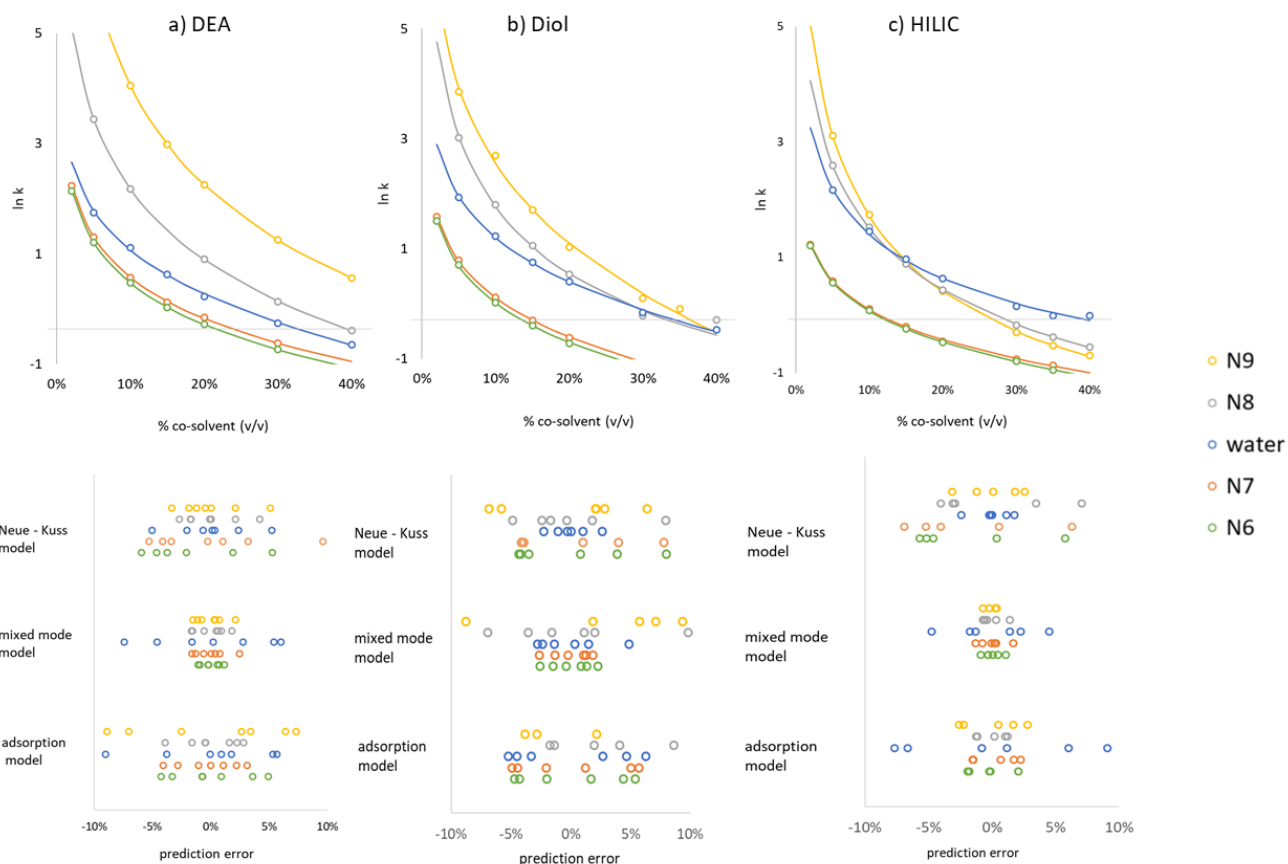
Table S1: Selected test compounds and associated composition at elution for different co-solvents. Column DEA, gradient 5 % to 50 % co-solvent, normalized gradient slope 2 %.



651  
 652 Figure S1: Change in peak variance for peaks N1-N3 eluting at initial mobile phase composition, for  
 653 various percentages of water in the ACN/ water diluent. Column DEA, co-solvent MeOH.  
 654  
 655  
 656  
 657  
 658



659  
 660 Figure S2: Injection solvent effect reported as change in peak variance for (a) N6 and (b) N10 vs. the  
 661 content of water in the diluent, the remaining solvent being acetonitrile (white marks) or methanol  
 662 (black marks).  
 663



664  
665

666 Figure S3: Retention relationships of water and four surrounding probes N6-N9. Ln k as a function of  
667 the MeOH content in mobile phase. Circles are experimental measurements based on isocratic runs.  
668 Plain lines are the associated prediction using mixed-mode model. Below are the associated  
669 prediction errors of three models. Percentage errors defined as  $(k_{\text{predicted}} - k_{\text{exp}})/k_{\text{exp}}$ . Columns (a)  
670 Torus DEA, (b) Torus diol and (c) BEH HILIC.

671  
672

673 **Equations for**

674 Neue-Kuss model 
$$\ln k = \ln k_0 + 2 \ln(1 + S_2 \phi) - \frac{S_1 \phi}{1 + S_2 \phi}$$

675 Mixed-mode model 
$$\ln k = \ln k_0 + S_1 \phi + S_2 \ln \phi$$

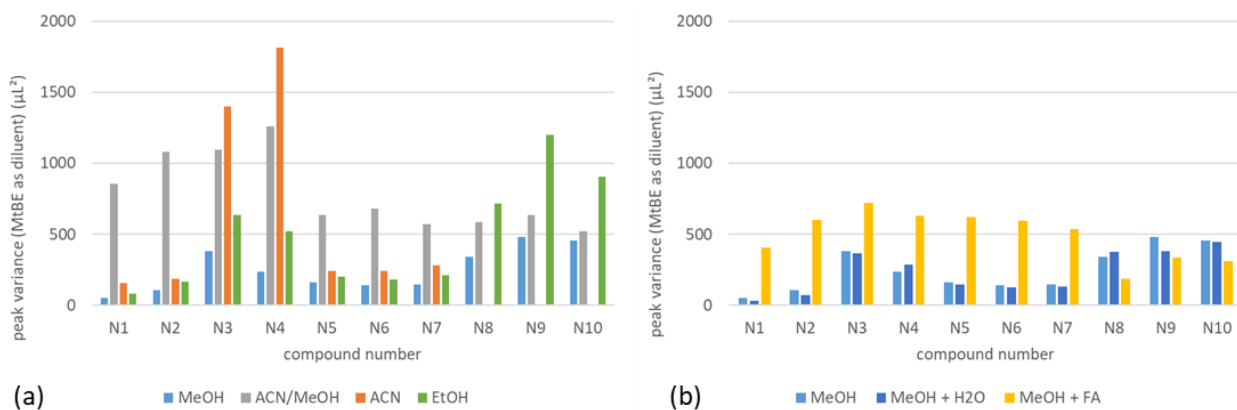
676 Adsorption model 
$$\ln k = \ln k_0 - S_1 \ln \phi$$

677

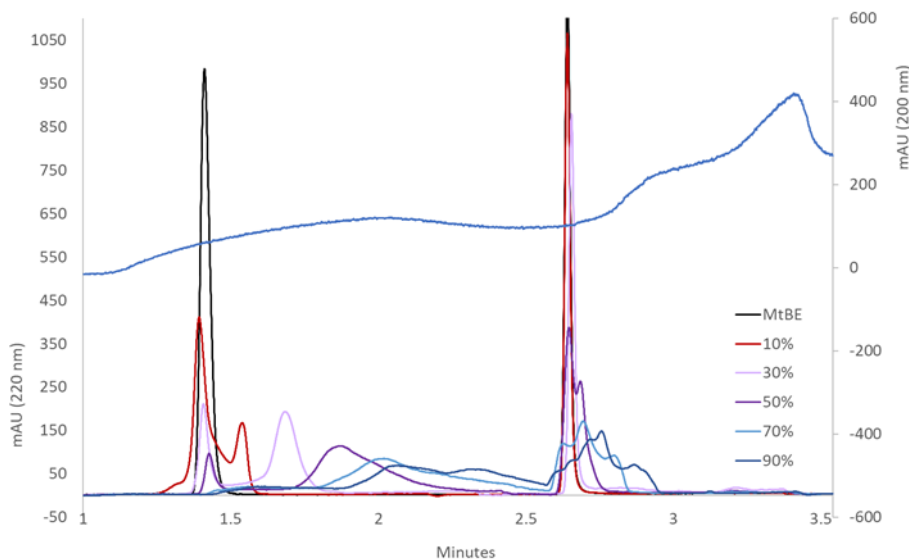
678 where  $\phi$  is the volumetric fraction of co-solvent,  $k_0$  the extrapolated value of k for  $\phi = 0$  (i.e., pure  $\text{CO}_2$ ),  
679  $S_1$  the slope and  $S_2$  the curvature coefficient.

680  
681  
682  
683  
684  
685  
686

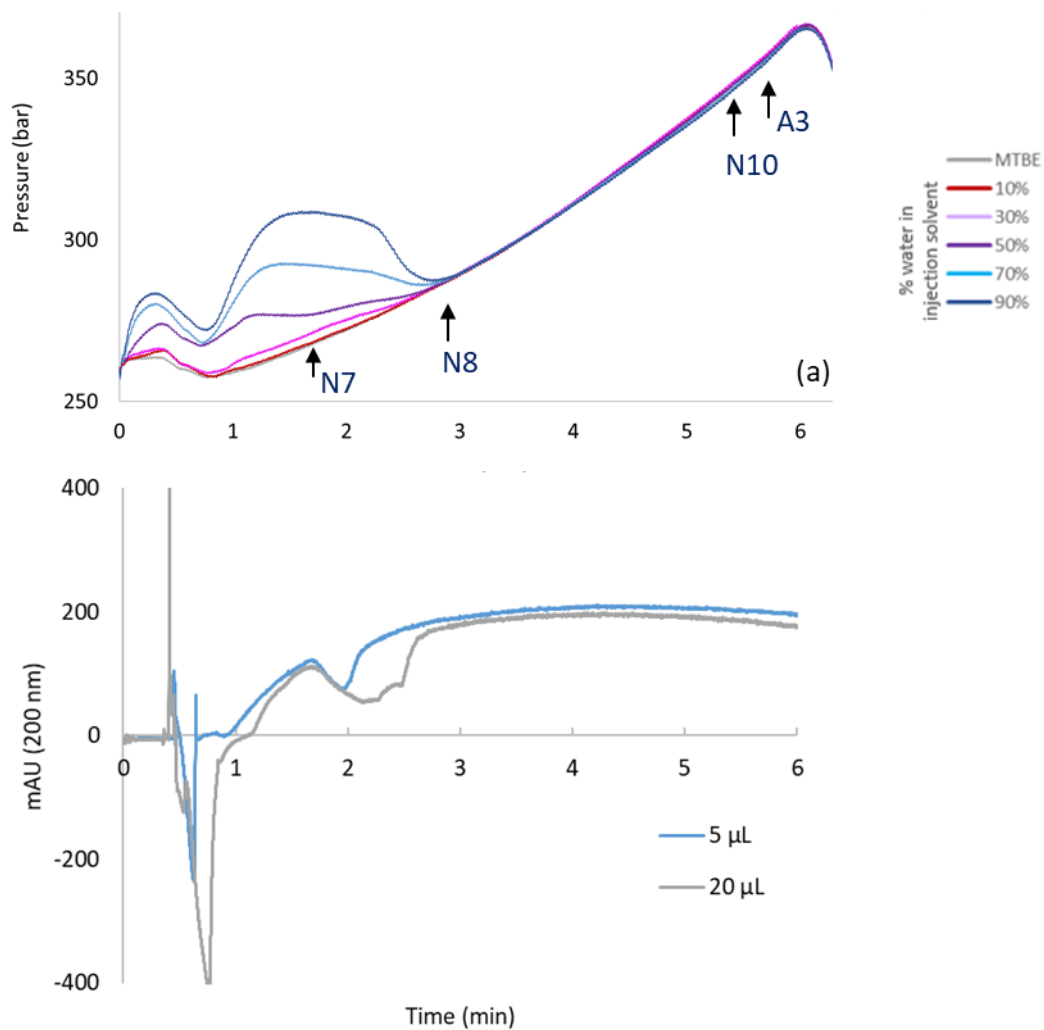




687 (a) MeOH ACN/MeOH ACN EtOH  
 688 (b) MeOH MeOH + H<sub>2</sub>O MeOH + FA  
 689 Figure S4: Peak variance of the neutral test compounds, using MtBE as diluent, (a) for various organic  
 690 co-solvents and (b) using MeOH with additives, i.e. 2 % water or 0.1 % formic acid additives as co-  
 691 solvent. Compounds N8-N10 were not eluting during the gradient when using ACN as co-solvent.  
 692



693 (a) MtBE  
 694 10%  
 695 30%  
 696 50%  
 697 70%  
 698 90%  
 699  
 700 Figure S5: (a) Chromatograms of two basic probes injected in ACN/water diluent with increasing  
 696 content of water. UV detection 220 nm. (b) UV trace of pure water. UV detection 200 nm.  
 697 Column DEA. Co-solvent MeOH + 2 % water + 20 mM ammonium hydroxide.



701  
 702  
 703  
 704  
 705  
 706  
 707  
 708

Figure S6: a) SFC inlet pressure when injecting 20  $\mu\text{L}$  ACN/water with increasing content of water and  
 b) System peaks recorded at 200 nm, when injecting 5  $\mu\text{L}$  and 20  $\mu\text{L}$  pure water. Column DEA. Co-  
 solvent MeOH. Other conditions stated in text.

709  
710  
711  
712

Table S1: Selected test compounds and associated composition at elution for different co-solvents.  
Column DEA, gradient 5 % to 50 % co-solvent, normalized gradient slope 2 %.

Compound	Co-solvent	Composition at elution (% co-solvent)						
		MeOH	ACN/MeOH 50/50	ACN	EtOH	MeOH + 2 % H <sub>2</sub> O + 0.1 % FA	MeOH	
eugenol	N1	5.0	5.0	5.0	5.0	5.0	5.0	
2,4,6 trimethylphenol	N2	5.0	5.0	6	5.0	5.0	5.0	
1-indanol	N3	5.0	5.7	7	5.6	5.0	5.0	
apocynin	N4	6.3	7.1	11	7.4	6.5	6.3	
o-cresol	N5	7.5	8.7	14	8.8	7.3	7.5	
m-cresol	N6	8.0	9.5	16	9.4	7.8	8.1	
phenol	N7	8.5	9.9	17	9.8	8.4	8.5	
4-hydroxybenzyl alcohol	N8	17.9	36.6	21.2	20.5	18.0	18.1	
naringenin	N9	28.7	Over	31.8	32.0	27.4	28.7	
arbutin	N10	35.3	Over	42.2	38.9	34.7	35.9	
Acidic	acrylic acid	A1	21.4	29.7	Over	31.3	20.8	17.4
	trans cinnamic acid	A2	26.7	34.8	Over	37.6	25.2	19.1
	ferulic acid	A3	37.0	43.6	Over	Over	35.8	29.6
Basic	imipramine	B1	6.4	N.D.	N.D.	N.D.	N.D.	N.D.
	propranolol	B2	15.4	N.D.	N.D.	N.D.	N.D.	N.D.
	Water		13.7	13.5	N.D.*	15.6	13.9	12.3

713  
714  
715  
716  
717  
718

N.D.: not determined

Over: retention over the gradient range (> 50 % co-solvent)

\*The water peak could not be detected at 200 nm due to the lack of UV absorbance of ACN co-solvent.